

LWP ITF Epoch 1992

Michele D. De La Peña and Bruce T. Coulter
Computer Sciences Corporation / IUE Observatory

I Introduction

This report discusses the criteria employed in the creation of the LWP Intensity Transfer Function (ITF) (Epoch 1992) and the determination of the corresponding effective exposure times.

One hundred thirty-three images were obtained for the LWP ITF during the marathon ITF acquisition effort from 26 April – 06 May 1992. For a majority of this eleven day period, the spacecraft was maintained in a stable configuration with respect to attitude and head amplifier temperature (THDA) in an effort to minimize changes in any physical parameters which could affect the quality of the UV Flood images. This stable environment was particularly important since for the IUE Final Archive image processing system, the ITF summed images are created in their own raw space in order to avoid resampling (smoothing) of the data. This requires that the images be geometrically similar to one another upon acquisition. As the THDA is known to correlate well with the geometric distortion of images (Bushouse 1991), it was necessary to obtain the images within a restricted range in THDA in order to maximize the likelihood that the images would co-align well. See Pérez et al. for a complete description of the acquisition procedures for the ITF images.

II Selection of Images for the ITF

All of the images were visually inspected for consistency and to catalog cosmic ray hits, missing minor frames, and permanent detector blemishes. This information is particularly useful in the determination of a pixel exclusion parameter used during the creation of the mean ITF level. This parameter is employed to exclude transient artifacts from the mean ITF image which may be present in an individual constituent image, while maintaining the noise characteristics of the data. The sophisticated averaging technique, used in the creation of the IUE Final Archive ITFs, allows images with some missing minor frames still to be utilized for their useful data that can contribute to the ITFs, in contrast to the summation procedures used for the IUESIPS ITFs.

The main criteria used to determine the suitability of an individual LWP exposure to be included as part of the ITF image were *image geometric registration* and *raw data number (DN) consistency* among the images acquired for an ITF level. These two criteria were used in tandem, and if necessary, iteratively. All of the images of a particular exposure level were cross correlated against a chosen representative image of that level to determine the general registration consistency, taking care that the reference image was not unusual. Depending upon the results of the registration analysis, multiple iterations of correlations using alternative references were performed until the best alignment for the majority of images was achieved.

The images selected by this method were then evaluated with respect to their DN consistency. A histogram of the entire illuminated portion of each image was computed, and an inter-comparison of the image histograms was used to determine the extent of agreement. The global histograms were considered to be a statistically reliable means of characterizing the image intensity without spatial bias. The agreement between the individual images in the ITF about the mean DN of an ITF level is $\pm 5\%$, and the maximum spread in DN from the "high" end image to the "low" end image is $\pm 7\%$. Figure 1 is a diagram illustrating the median DN value, as determined from the image histograms, of *all* the LWP images acquired for the ITF; Figure 2 is a diagram depicting the median DN value of the images chosen as constituent images for the LWP ITF (Epoch 1992). In these diagrams, each short horizontal line may represent one or more images depending upon the determined median DN value associated with the image. The lines have been extended horizontally for clarity of the presentation, but actually represent one ITF level each. The solid curve connects the median DN value of each ITF level. Table 1 lists basic information for each level of the LWP ITF. The determination of the effective exposure time in this table is described below. Tables 2 *a - e* document more specific information regarding all of the individual images acquired for possible use in the ITF. Each image obtained for the ITF is listed with the associated ITF level (1 - 12) and percent exposure (the percentage of counts in the current exposure as compared to an optimum reference exposure, where the reference is defined to be 100%). MEDIAN XCC represents the median cross correlation coefficient determined for the specific image with respect to the REFERENCE image for the level using a linear cross correlation algorithm; the median is determined from the 490 image positions tested. The REFERENCE image for each level is indicated by REF in the MEDIAN XCC column. As the cross correlation technique is a pattern matching algorithm, this parameter indicates the degree of similarity between the respective images from a geometric perspective. MEAN SHIFT is the average displacement between the current image and the REFERENCE as computed from the 490 image positions tested. The THDA is the temperature at the end of the exposure of the camera head amplifier. The checkmark in the final column indicates that the image was used in the creation of the ITF. See Nichols et al. for a complete description of the cross correlation algorithm and analysis parameters.

Table 1: LWP ITF (Epoch 1992)

Level	Median DN of Level	# of Acquired Images	# of Images Used	Effective Exposure Time (s)
1	25.5	18	9	0.000
-	38.0	1	0	-
2	49.7	10	8	38.750
3	75.7	8	8	78.737
4	103.5	8	8	121.868
5	128.2	34	13	168.958
6	146.8	9	6	200.756
7	164.2	7	6	237.941
8	182.4	8	6	278.107
9	210.8	9	4	341.073
10	229.1	8	5	396.582
11	251.1	7	5	483.497
12	254.6	6	4	561.518

The selection of images for an ITF level is a balance of the registration accuracy, DN consistency, and the desire for a high signal-to-noise ratio (S/N) in the mean level. The registration accuracy is necessary to ensure, on a pixel-by-pixel basis, the proper averaging of information without spatial blurring of the inherent fixed pattern. The DN consistency is required to guarantee: all of the images truly represent a "parent" ITF level, the images do not overlap with the adjacent levels, and to eliminate the blurring of the fixed pattern in intensity. Finally, it is desirable to average as many suitable images as are available to obtain the highest possible S/N in the ITF, as it represents the ultimate limit of the S/N achievable in the science data.

III Geometric Dichotomy in the ITF Data

During the examination of the registration characteristics of the images acquired for the new ITF, it became apparent for the levels that had a large number of images (Null and 80%) that the images divided approximately evenly into two geometric groups. The distinctiveness of these subgroups is surprising and most evident in the Null exposures (henceforth referred to as Null A and Null B). While there exists some expected displacement between either Null and the 20% level of the ITF, neither the magnitude nor the direction of either displacement was sufficient to eliminate the use of one the Nulls. However, the geometric consistency of Null A and Null B with the science images shows an obvious difference in the character of the Nulls. Figure 3 plots the median correlation coefficient versus observation date for LWP Sensitivity Monitoring images as registered against Null A (asterisk symbols) and Null B (square symbols). As sensitivity monitoring images are short exposures, the Null image will generally be used for registration purposes as the ITF level most similar to the background of the science image in intensity.

It was determined by Bushouse (1991) that the median cross correlation coefficient (R) for an image (where the magnitude of the coefficient reflects the confidence level of the image registration between the raw science image and the ITF) is a useful indicator of the relative S/N that will be achieved in the final NEWSIPS extracted spectrum. In this context correlation coefficients range from 0.0 (no correlation) to +1.0 (a perfect correlation), and the larger the correlation coefficient, the better the registration and the higher the S/N in the extracted spectrum. The strength of the median correlation coefficient is modulated by changes in the fixed pattern fiducial in the raw science image relative to the ITF. Consequently, if the fixed pattern has evolved over time, the pattern match between the ITF and a raw science image containing an evolved pattern will result in a reduced confidence and the correlation will be weak.

Although Null B was shown to be geometrically more appropriate to the majority of the LWP science data (post-1984) than Null A, the DN level of Null B is higher than that of not only Null A, but also a large fraction of low intensity science exposures. This slightly high DN plateau of Null B does not allow this Null to bracket appropriately

the low end of the ITF, and in fact manifested this characteristic by producing many negative extrapolations in the science data. Null A exhibits registration improvement over the Null of the LWP ITF (Epoch 1984) and possesses an appropriate DN level for the shortest exposure science data. Consequently, Null A was chosen to be the Null level of the LWP ITF (Epoch 1992).

We were driven by the requirements that the Final Archive processing system be fully automated and the IUE archive be uniformly processed. These requirements provided no opportunity for the use of both Null A and Null B in the processing, with the selection based on the geometric registration and background DN level of each science image. However, as is clearly seen in Figure 3, many images with long exposure times (thus not subject to the negative extrapolation problem) would have better registration with an ITF constructed with Null B, and consequently better S/N in the extracted spectral data. An ITF constructed with Null B and the associated effective exposure times is available and will be archived. However, no absolute flux calibration or sensitivity degradation correction will be available.

IV Derivation of the Effective Exposure Times

The ITF is used to linearize and normalize the raw intensity values, and to accomplish this successfully, the ITF levels need to be discrete and the relative exposure of the levels understood, particularly at the highest levels of the ITF where saturation effects make it difficult to characterize the data properly. The most straightforward relationship to establish is one between exposure time and the median DN of the images. However, this relationship is complicated by degradation of the UV flood lamp output. Because the UV Flood lamps degrade with usage, for a given commanded exposure time the lamp output will decrease with respect to a preceding reference image; this decline is manifested as a decrease in the DN level of the exposure. During the acquisition of an ITF, the lamps are heavily utilized over a relatively short period of time, and this degradation is particularly noticeable. To model the lamp output degradation, exposure meter images were taken frequently during the ITF acquisition, allowing the degradation to be modeled. From the model, effective exposure times were derived for the ITF images which are indicative of the DN level of the image.

The calculation of the effective exposure times for the ITF images is a multi-stage process which depends upon a well-determined null level (Holm 1983, Imhoff and Scott 1985). The null level of the ITF is critical for three reasons:

- The null pedestal must be subtracted from the exposure meter images in order to compute the lamp efficiency function during the ITF sequence.
- The null pedestal is effectively subtracted from all science images during the photometric correction procedure.

- The null most closely matches in DN the background intensity of a majority of the science images, and therefore, this level will be used a majority of the time to determine geometric distortion.

Due to the importance of the null exposures, they were carefully checked for any correlation with the previous exposure or THDA. No correlations were found for these images.

The LWP exposure meter images, 80% exposures, were obtained approximately every 5th exposure to provide the baseline with which to track the lamp degradation. In contrast to the previous ITF image acquisition sequences, the commanded exposure times for all ITF images acquired for the 1992 ITF were modified in real time to maintain the desired DN levels. This dynamic change in the exposure times was possible due to continuous monitoring and immediate analysis of the UV Flood images as they were read down from the spacecraft.

The lamp efficiency, E_i , was derived from the following equation,

$$E_i/s = \left[\frac{DN(80_i) - DN(Null_{ITF})}{DN(80_{ITF}) - DN(Null_{ITF})} \right] / cte_{xp_i} \quad (1)$$

where the efficiency was computed per second to account for the changes in the commanded exposure time. $DN(80_i)$ is the median DN of the i th exposure meter image; $DN(Null_{ITF})$ is the median DN of the null level of the ITF; $DN(80_{ITF})$ is the median DN of the 80% level of the ITF; and cte_{xp_i} is the commanded exposure time of the i th exposure meter image, corrected for the on board computer quantification of the up-linked exposure time ($obctic$) and the camera rise time (Oliversen 1991). The median DN used to characterize an image was computed from the histogram of all pixels within the illuminated portion of the target. E_i/s was then normalized to range from 0.0 to 1.0, plotted against the independent variable of chronological date of exposure, and fit with a quadratic function as seen in Figure 4. The efficiency function was computed using all of the exposure meter images, not only the images that were chosen to be constituents of the ITF. The square symbol denotes the preliminary exposure meter image which was not used in the computation of the fitting function. This preliminary exposure meter image taken during the ITF sequence was based upon an estimate of the exposure time required to obtain the desired DN level; the exposure time was immediately adjusted from this initial estimate. The three exposure meter images acquired on Day 127, represented by the triangle symbol, were necessarily displaced -3 days to be adjacent in time to the previous LWP UV Flood exposures as explained below.

Although the lamp degradation function for earlier ITF epochs was derived as a function of chronological time, the degradation has a more direct relationship with lamp usage expressed as cumulative exposure time. Figure 5 depicts this relationship which has been fit with a linear function. As in Figure 4, the square symbol represents preliminary data not used to determine the fitting function. Based upon this relationship with lamp

usage, the last three data points align with the remaining data naturally. During Days 124 – 126, the LWP UV Flood lamp was not utilized. It should be noted that the flood lamps are actually firing for a longer period of time than the length of the exposure. Technically, this “firing” time is a function of both the RAW(AS3CH31) value which is *uplinked* at the execution of the scientific payload procedure (ITF PROC) and the *current* value of RAW(AS3CH31); this parameter is inversely proportional to the temperature of the flood lamp. Despite rigorous data recording procedures, all of these values are not available for analysis. However, due to the agreement between the two described degradation determinations (as discussed in the next paragraph), the lamp degradation has been well modelled with the current available information.

Although the derived lamp output correction factors based upon lamp degradation versus lamp usage (fit with a linear function) are different than those based upon the degradation versus chronological time (fit with a quadratic function), the effective exposure times ultimately derived for all of the UV Flood lamp exposures are consistent between the two methods. However, the lamp degradation versus lamp usage as modelled by a linear fit was chosen to define the correction factors as this function is based upon a causal relationship, and the data adhere naturally to the model.

Once the degradation was modelled, the effective exposure time for each individual UV Flood image was computed by multiplying the commanded exposure time, corrected for obctc quantization and camera rise time, by the defined correction factor. Consequently, the “mean” effective exposure times for each ITF level were then computed by averaging the exposure times corresponding to the constituent images per level. The mean exposure times and median DN values for the twelve levels define a “representative” ITF as depicted in Figure 6.

This “ITF” was used to refine the derived effective exposure times by first converting the median DN values of the exposure meter images into FNs, and then refitting the lamp degradation (now based upon normalized FN data) versus lamp usage with a linear function. This second iteration efficiency function changed little from the first approximation. Finally, the refined efficiency function was utilized to re-determine the effective exposure times for all of the UV Flood images, and ultimately, the new, mean effective exposure times for the ITF levels. For illustration, this second generation ITF was used to convert the median DNs of all the LWP UV Flood exposures into FNs and plotted in Figure 7.

V Geometric Comparison of the LWP ITFs

Figure 8 shows the median correlation coefficient, R , for the LWP sensitivity monitoring images as a function of time (observation date), utilizing the LWP ITF (Epoch 1984) (square symbols) and the LWP ITF (Epoch 1992) Null A (asterisk symbols) as the

respective registration guides. The vertical dashed lines represent the times at which the LWP ITF (Epoch 1984) and the LWP ITF (Epoch 1992) Null A were obtained. For this dataset, the LWP ITF (Epoch 1992) Null A yields an improvement in the overall confidence of the image registration for data obtained after mid-1984. Post-1984 is the beginning of the time period when the majority of the LWP science images have been obtained.

Figure 9 depicts the amount of misregistration for a chosen LWP sensitivity monitoring image versus the 1984 and 1992 LWP ITFs. The misregistration illustrates the displacement of the fixed pattern between the science image and the ITF. The noticeable lack of displacement between the science image and the LWP ITF (Epoch 1992) indicates a strong geometric similarity between the images and is one demonstration of the appropriateness of the 1992 ITF. Figure 10 illustrates the strength of the correlation as indicated by the size of the "+" symbol. The amount of improvement in the registration confidence using the LWP ITF (Epoch 1992) is distinctive - particularly in the LWP "noisy patch" which corresponds to the short wavelength portion of the LWP data (upper right part of the bounded circle).

VI References

- Bushouse, H.A., 1991, *Record of the IUE Three Agency Coordination Meeting*, CSC/TM-91/6163, D-17.
- Holm, A., 1983, IUE Internal Memorandum.
- Imhoff, C.L., and Scott, E.H., 1985, *Record of the IUE Three Agency Coordination Meeting*, CSC/TM-86/6114, S-2.
- Nichols, J.S., Garhart, M.P., De La Peña, M.D., and Levay, K.L., 1993, *International Ultraviolet Explorer New Spectral Image Processing System Information Manual: Low-Dispersion Data, Version 1.0*, CSC/SD-93/6062.
- Oliversen, N., 1991, *NASA IUE Newsletter*, 45, 56.
- Pérez, M., Nichols-Bohlin, J., De La Peña, M., Bushouse, H., Garhart, M., and Groebner, A., 1992, *NASA IUE Newsletter*, 48, 65.

Table 2a: Images Taken in 1992 for Development of a New LWP ITF

Image Number	ITF Level	% Exp.	Median XCC	Mean Shift	THDA	Used in ITF (✓)
22903	1	NULL	REF	0.000	9.17	✓
22910	1	NULL	0.955	0.029	8.50	✓
22911	1	NULL	0.921	0.073	8.50	
22925	1	NULL	0.875	0.068	7.16	✓
22926	1	NULL	0.915	0.051	7.16	
22932	1	NULL	0.909	0.069	9.51	✓
22933	1	NULL	0.940	0.045	9.51	✓
22956	1	NULL	0.931	0.041	9.17	✓
22979	1	NULL	0.772	0.191	9.84	
23000	1	NULL	0.922	0.049	8.84	✓
23001	1	NULL	0.878	0.122	9.17	
23002	1	NULL	0.831	0.156	9.51	
23006	1	NULL	0.938	0.053	8.84	✓
23011	1	NULL	0.868	0.128	9.17	
23015	1	NULL	0.875	0.118	9.17	
23019	1	NULL	0.869	0.125	9.17	
23037	1	NULL	0.951	0.025	8.84	✓
23043	1	NULL	0.884	0.086	9.17	
22927		10	REF	0.000	6.49	
22913	2	20	0.810	0.050	8.17	
22935	2	20	REF	0.000	9.51	
22948	2	20	0.830	0.037	10.18	✓
22964	2	20	0.836	0.044	10.18	✓
22975	2	20	0.842	0.025	9.84	✓
22984	2	20	0.828	0.042	9.84	✓
22992	2	20	0.842	0.045	10.18	✓
22998	2	20	0.827	0.049	9.84	✓
23016	2	20	0.847	0.033	9.17	✓
23034	2	20	0.837	0.039	9.84	✓

Table 2b: Images Taken in 1992 for Development of a New LWP ITF

Image Number	ITF Level	% Exp.	Median XCC	Mean Shift	THDA	Used in ITF (✓)
22922	3	40	0.778	0.037	8.17	✓
22945	3	40	0.766	0.055	10.51	✓
22960	3	40	REF	0.000	9.51	✓
22970	3	40	0.801	0.032	9.84	✓
22982	3	40	0.801	0.035	9.51	✓
22987	3	40	0.796	0.043	9.84	✓
22995	3	40	0.787	0.046	9.84	✓
23027	3	40	0.796	0.034	9.17	✓
22917	4	60	0.774	0.044	8.17	✓
22937	4	60	REF	0.000	9.51	✓
22953	4	60	0.773	0.047	10.18	✓
22966	4	60	0.790	0.032	9.84	✓
22977	4	60	0.782	0.042	9.84	✓
23009	4	60	0.783	0.036	8.84	✓
23022	4	60	0.787	0.032	9.17	✓
23032	4	60	0.783	0.040	9.51	✓
22904	5	80	0.812	0.023	9.17	
22905	5	80	REF	0.000	9.17	✓
22907	5	80	0.802	0.030	9.17	✓
22912	5	80	0.791	0.040	8.17	✓
22915	5	80	0.785	0.030	8.17	✓
22920	5	80	0.781	0.036	8.17	✓
22924	5	80	0.756	0.050	7.83	✓
22928	5	80	0.719	0.087	6.82	
22934	5	80	0.796	0.036	9.51	✓
22940	5	80	0.770	0.057	9.84	✓
22944	5	80	0.705	0.099	10.18	
22949	5	80	0.714	0.083	10.18	
22950	5	80	0.785	0.044	9.84	✓

Table 2c: Images Taken in 1992 for Development of a New LWP ITF

Image Number	ITF Level	% Exp.	Median XCC	Mean Shift	THDA	Used in ITF (✓)
22955	5	80	0.763	0.061	9.84	
22957	5	80	0.777	0.058	9.51	
22963	5	80	0.728	0.089	10.18	
22968	5	80	0.718	0.102	10.18	
22973	5	80	0.706	0.106	10.18	
22974	5	80	0.771	0.062	9.84	
22978	5	80	0.762	0.067	9.84	
22980	5	80	0.793	0.040	8.84	✓
22986	5	80	0.740	0.081	9.84	
22991	5	80	0.714	0.098	10.18	
22994	5	80	0.729	0.091	9.84	
22999	5	80	0.708	0.108	9.84	
23007	5	80	0.786	0.052	8.84	✓
23013	5	80	0.767	0.078	9.17	
23018	5	80	0.746	0.079	9.17	
23020	5	80	0.771	0.053	9.17	✓
23025	5	80	0.743	0.084	9.51	
23029	5	80	0.755	0.080	9.17	
23038	5	80	0.781	0.046	8.84	
23039	5	80	0.792	0.033	8.84	✓
23045	5	80	0.755	0.065	9.17	
22923	6	100	0.709	0.090	8.17	
22942	6	100	REF	0.000	10.18	✓
22962	6	100	0.800	0.025	9.84	✓
22976	6	100	0.794	0.026	9.84	✓
22989	6	100	0.795	0.033	10.18	
23012	6	100	0.769	0.047	9.17	✓
23028	6	100	0.770	0.053	9.17	
23030	6	100	0.771	0.050	9.17	✓
23031	6	100	0.761	0.052	9.17	✓

Table 2d: Images Taken in 1992 for Development of a New LWP ITF

Image Number	ITF Level	% Exp.	Median XCC	Mean Shift	THDA	Used in ITF (✓)
22916	7	120	0.752	0.068	8.17	
22939	7	120	REF	0.000	9.51	✓
22952	7	120	0.796	0.038	10.18	✓
22969	7	120	0.805	0.024	9.84	✓
22985	7	120	0.790	0.056	9.84	✓
22996	7	120	0.785	0.057	9.84	✓
23023	7	120	0.795	0.032	9.17	✓
22906	8	140	0.795	0.065	9.17	
22946	8	140	0.819	0.022	9.84	✓
22958	8	140	0.823	0.020	9.84	✓
22959	8	140	REF	0.000	9.84	✓
22972	8	140	0.803	0.044	9.84	✓
22988	8	140	0.804	0.044	10.18	
23010	8	140	0.777	0.055	8.84	✓
23014	8	140	0.799	0.037	9.17	✓
22919	9	170	0.746	0.099	8.17	
22936	9	170	0.783	0.079	9.17	
22954	9	170	0.826	0.036	9.84	✓
22965	9	170	REF	0.000	9.84	
22981	9	170	0.820	0.040	9.51	✓
22993	9	170	0.490	0.370	10.18	
23021	9	170	0.807	0.045	10.18	✓
23033	9	170	0.819	0.038	9.51	
23041	9	170	0.817	0.035	9.51	✓
22914	10	200	0.670	0.178	7.83	
22941	10	200	REF	0.000	9.84	✓
22947	10	200	0.848	0.035	10.18	✓
22971	10	200	0.843	0.042	9.84	✓
22997	10	200	0.807	0.101	9.84	
23017	10	200	0.807	0.084	9.17	
23040	10	200	0.815	0.082	9.51	✓
23044	10	200	0.817	0.068	9.17	✓

Table 2e: Images Taken in 1992 for Development of a New LWP ITF

Image Number	ITF Level	% Exp.	Median XCC	Mean Shift	THDA	Used in ITF (✓)
22921	11	240	0.816	0.112	8.17	
22938	11	240	REF	0.000	8.17	✓
22961	11	240	0.861	0.042	9.84	✓
22983	11	240	0.850	0.052	9.84	✓
23008	11	240	0.831	0.080	8.84	✓
23026	11	240	0.818	0.117	9.17	
23042	11	240	0.847	0.060	9.17	✓
22918	12	280	0.763	0.134	8.17	
22943	12	280	0.884	0.031	10.18	✓
22951	12	280	REF	0.000	9.84	✓
22967	12	280	0.873	0.044	9.84	✓
22990	12	280	0.839	0.090	10.18	
23024	12	280	0.847	0.064	9.51	✓

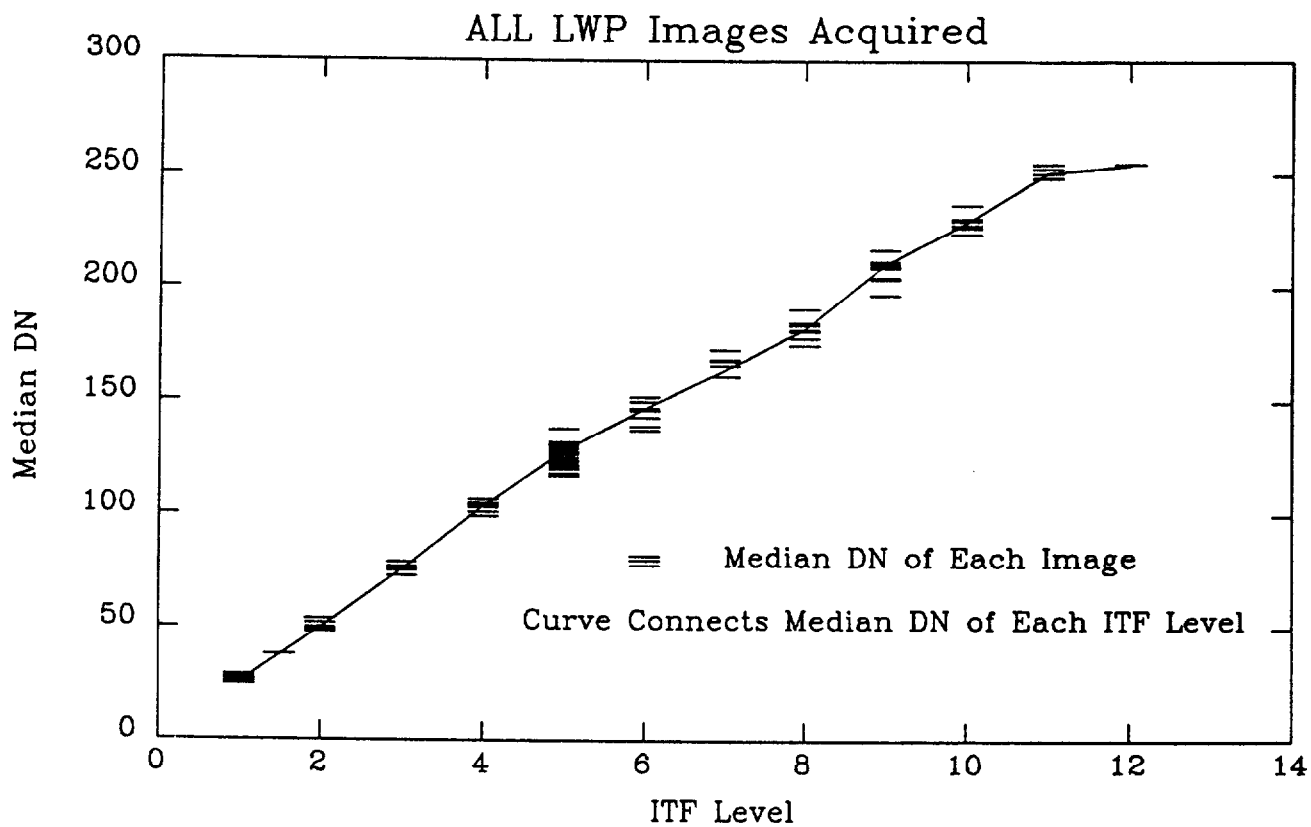


Figure 1

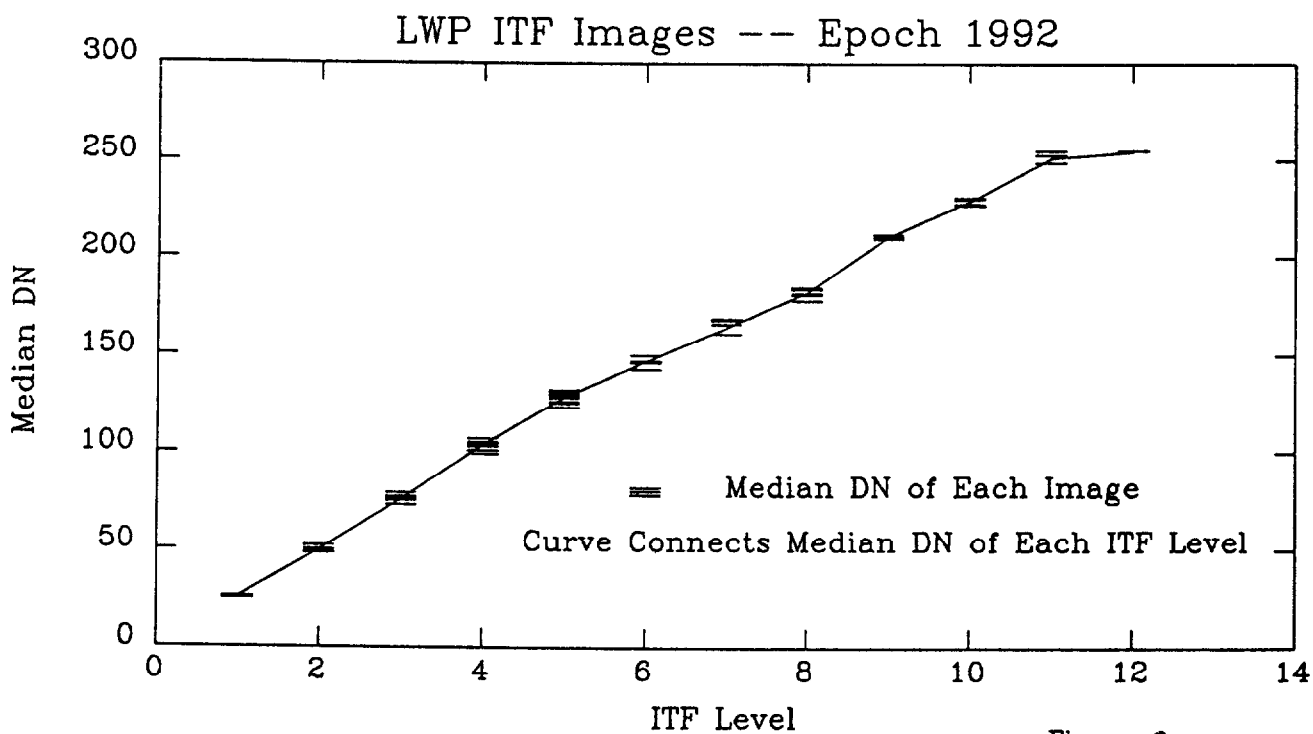


Figure 2

Sensitivity Monitoring Images

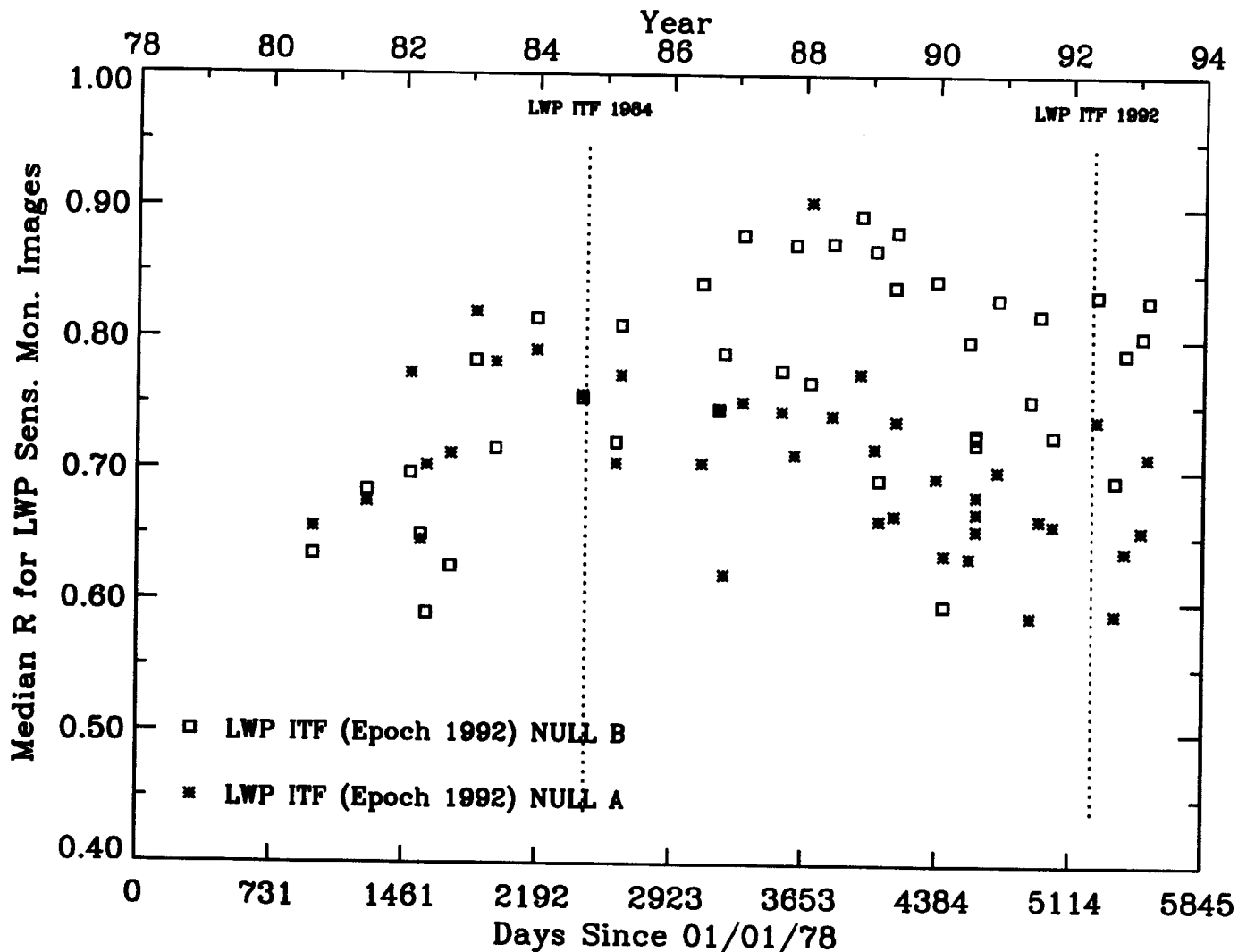


Figure 3

Figure 3. Comparison of the median correlation coefficients derived from registering the LWP Sensitivity Monitoring images against two different reference images: LWP ITF (Epoch 1992) Null A (asterisk symbol), and LWP ITF (Epoch 1992) Null B (square symbol).

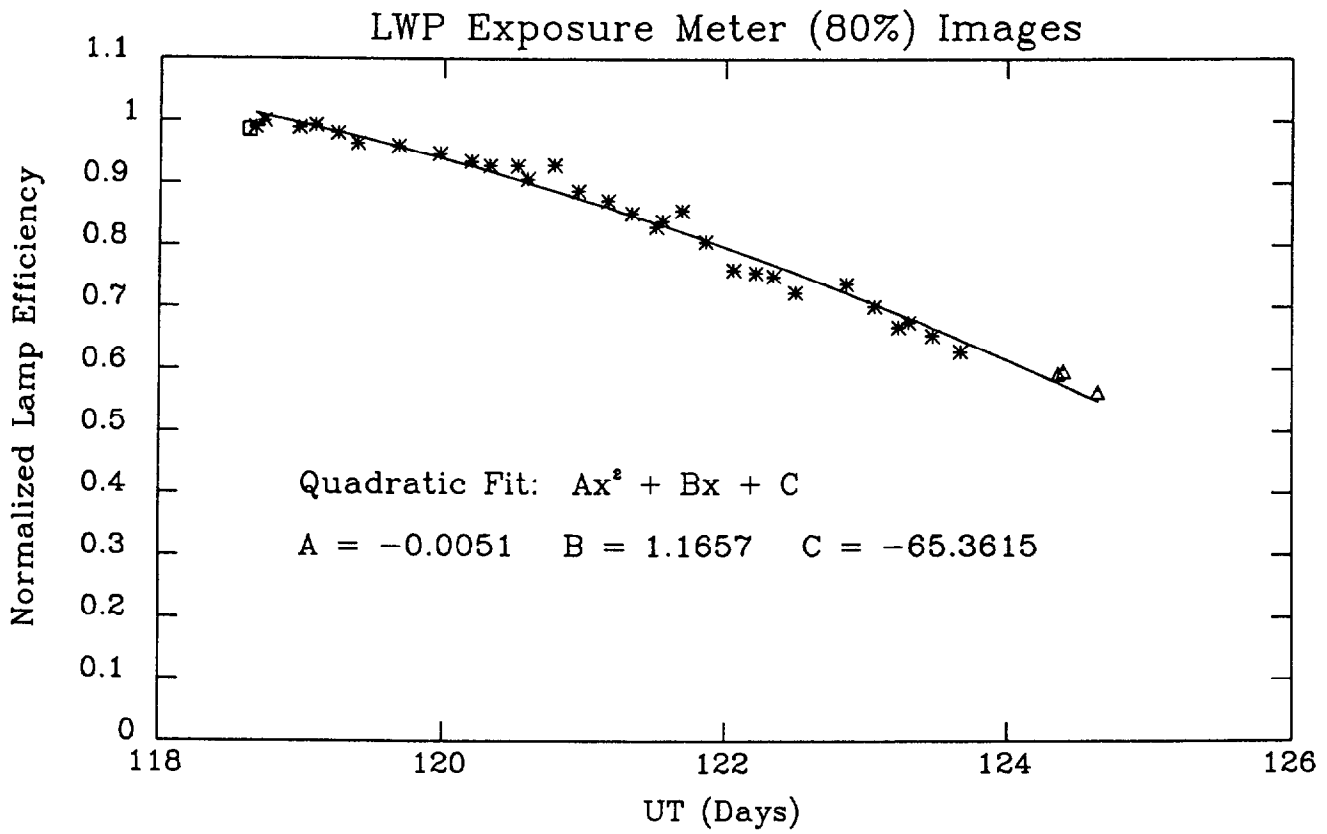


Figure 4

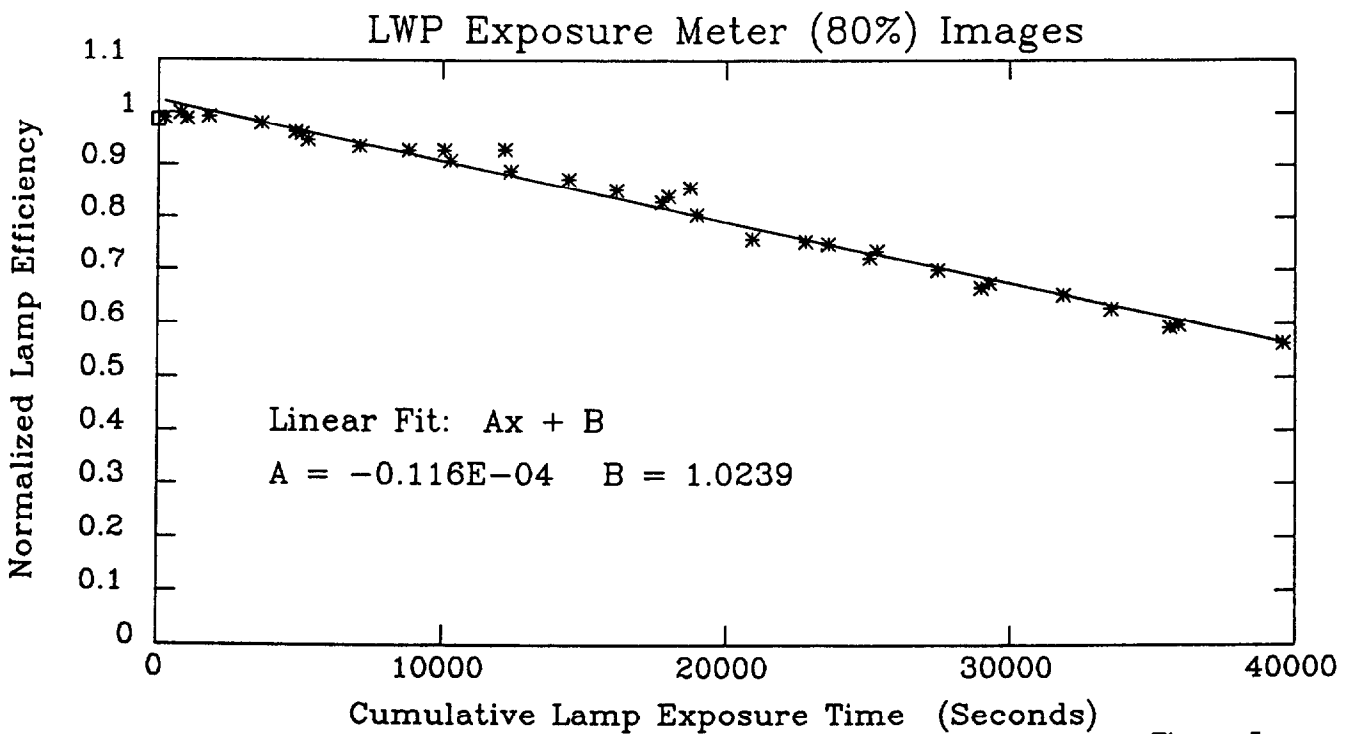


Figure 5

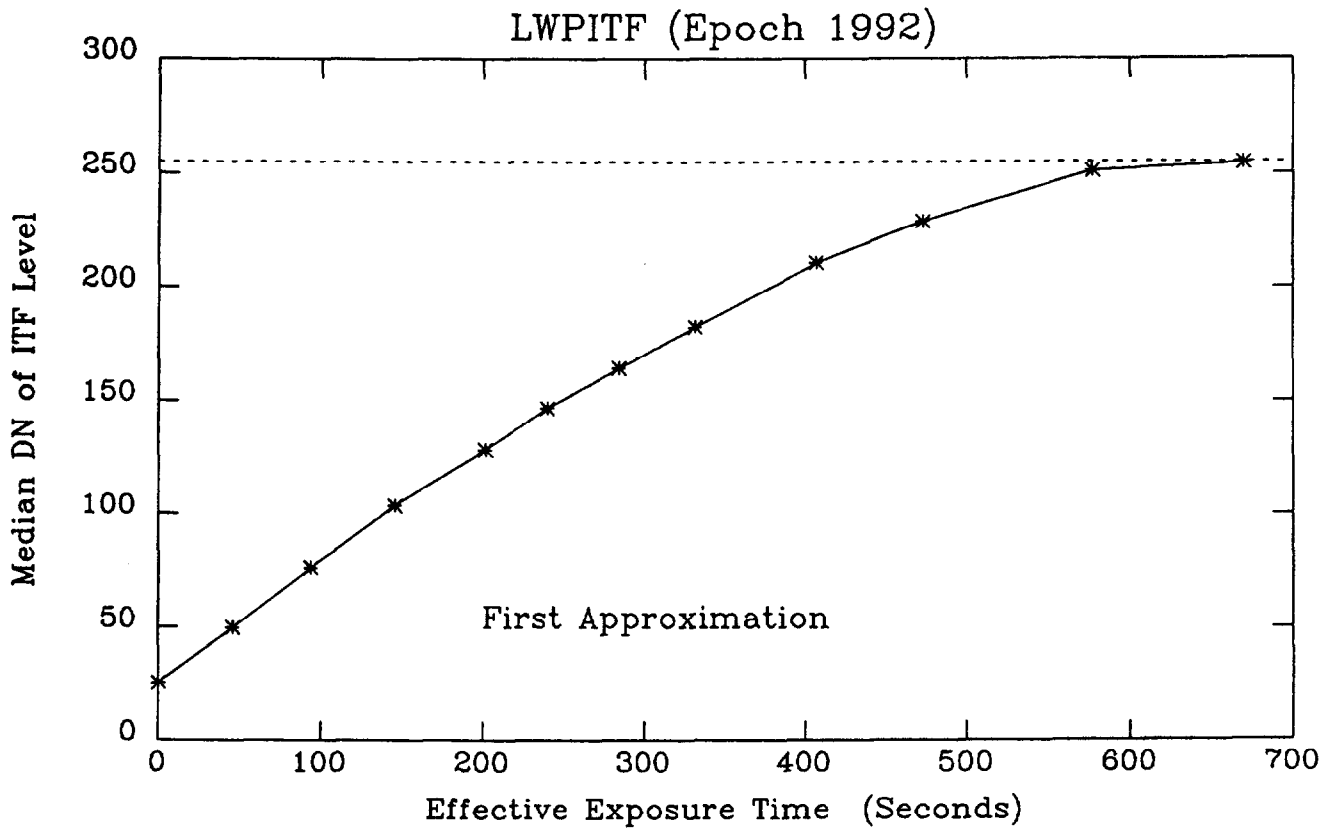


Figure 6

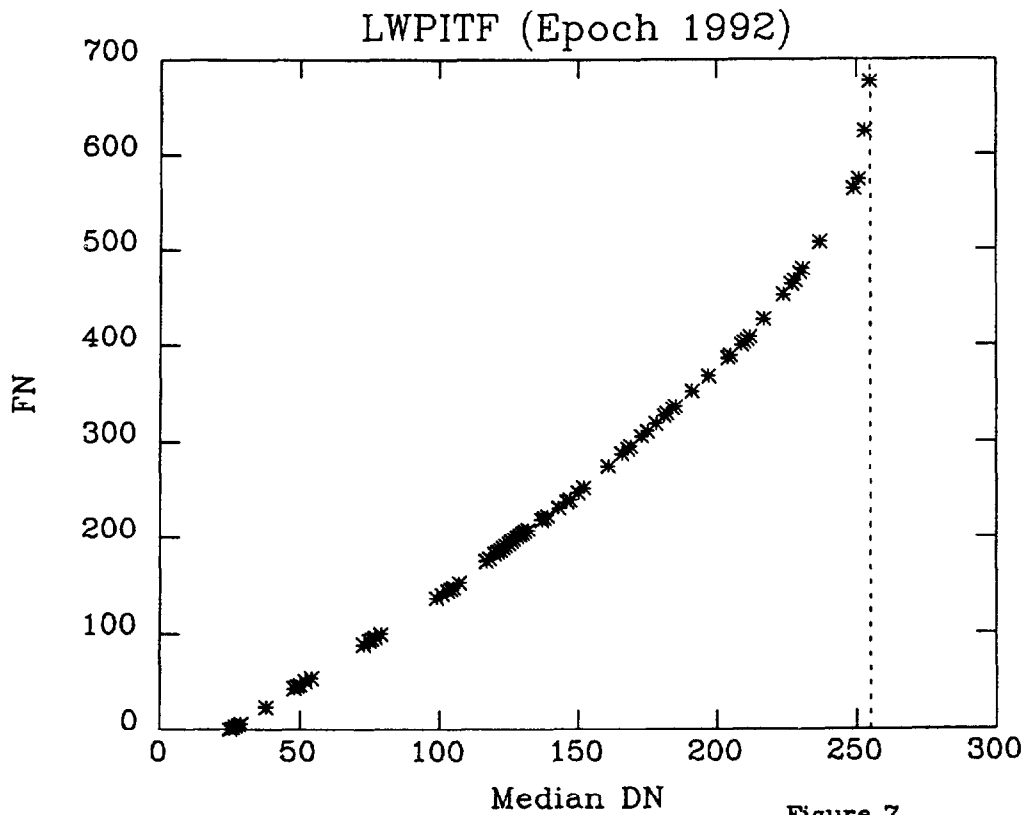


Figure 7

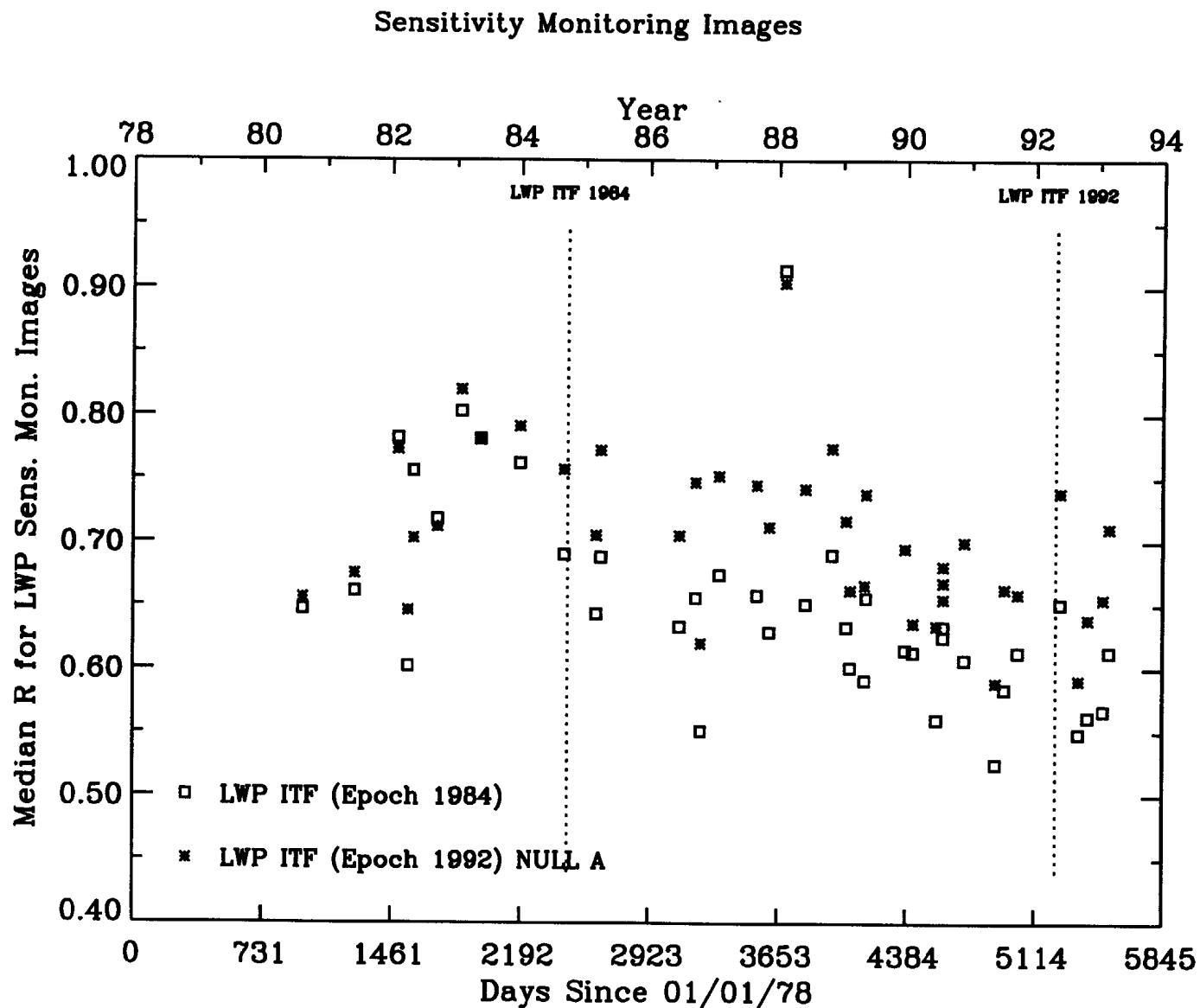


Figure 8

Figure 8. Comparison of the median correlation coefficients derived from registering the LWP Sensitivity Monitoring images against two different reference images: LWP ITF (Epoch 1992) Null A (asterisk symbol), and LWP ITF (Epoch 1984) (square symbol).

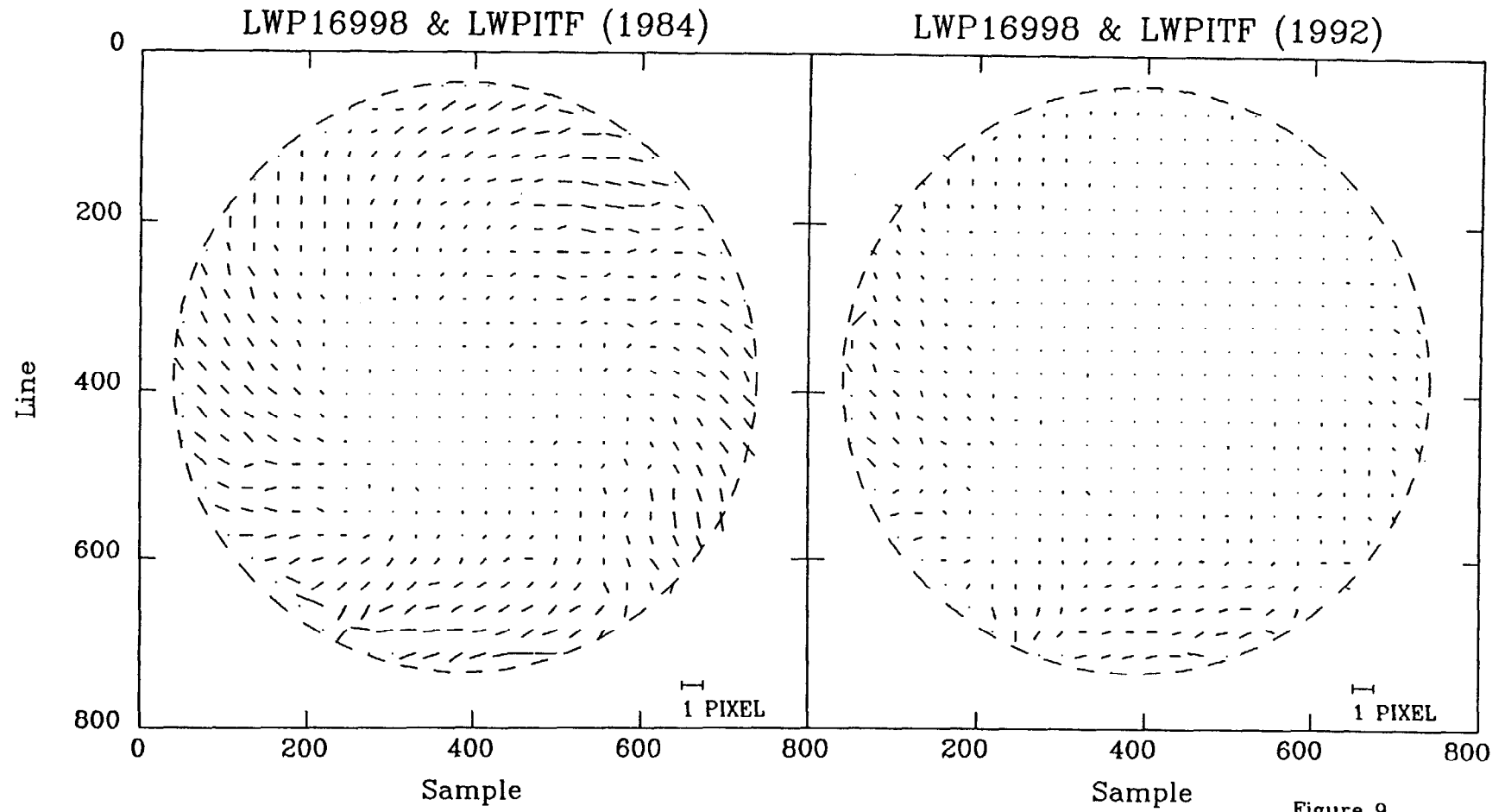


Figure 9

Figure 9. Displacement vectors derived between LWP16998 and two respective reference images: LWP ITF (Epoch 1984) and LWP ITF (Epoch 1992) Null A. Single dots represent positions of successful correlations. The associated vectors indicate the magnitude and direction of displacement between the science image and the reference image.

Correlation Strength

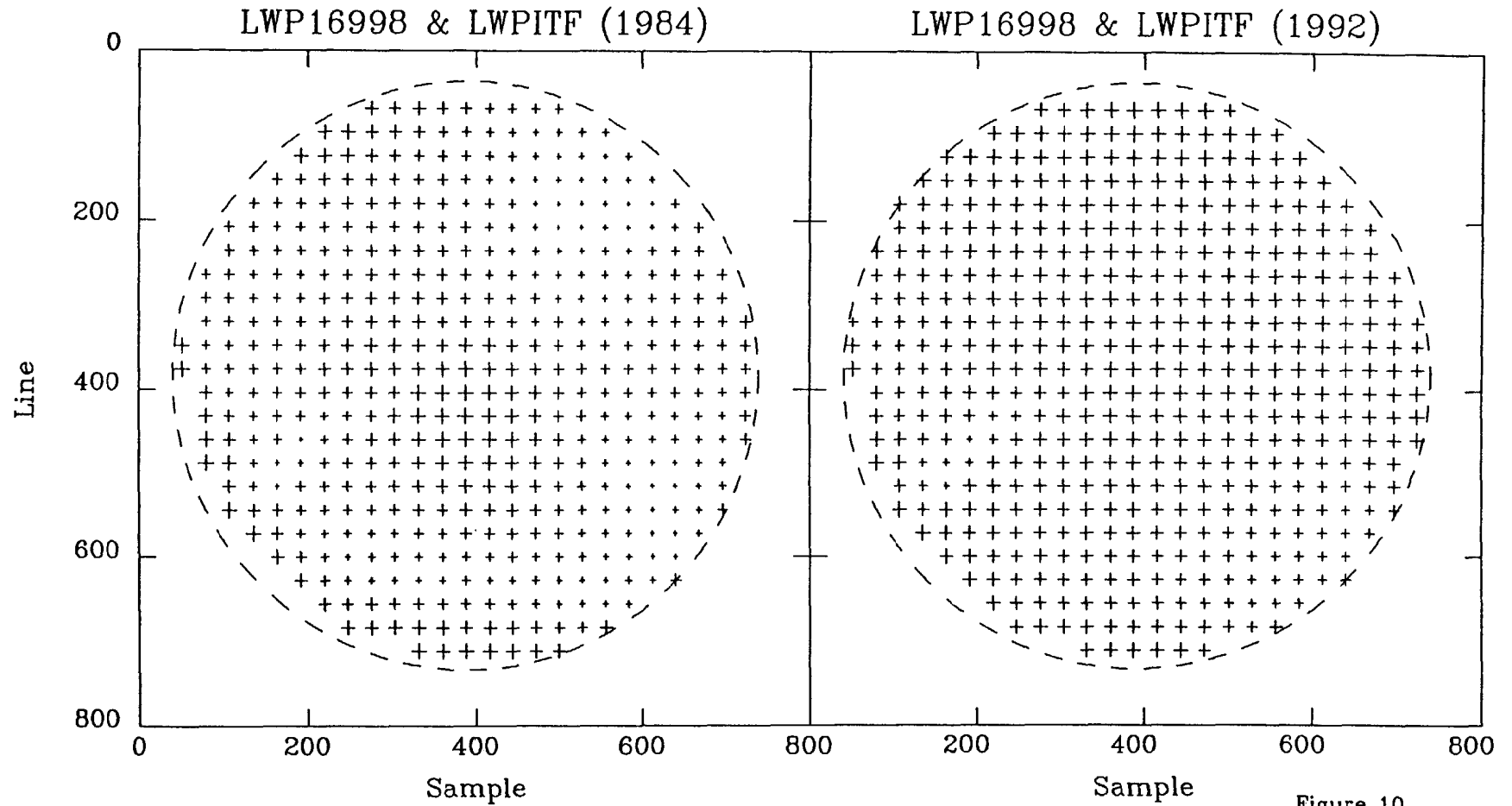


Figure 10

Figure 10. The “+” symbol is present for all locations where the cross correlation scheme is applied. The size of the symbol represents the strength of the correlation. In this context all correlations are positive and range between 0.0 (no correlation) and 1.0 (perfect correlation).